UCSF

UC San Francisco Electronic Theses and Dissertations

Title

Probing Integrin Specificity in regards to Clustering Dynamics on Soft and Stiff Matrices

Permalink

Author

Gile, Ryan Edward

Publication Date

2011

Peer reviewed|Thesis/dissertation

Probing Integrin Specificity in regards to Clustering Dynamics on Soft and Stiff Matrices

by

Ryan Edward Gile

THESIS

Submitted in partial satisfaction of the requirements for the degree of

MASTER OF SCIENCE

in

Biological and Medical Informatics

in the

GRADUATE DIVISION

Acknowledgments

Valerie Weaver, for serving as my graduate advisor, providing financial support, and encouraging me to follow my dreams.

Zena Werb, for useful input into this document.

Torsten Wittmann, for useful input into this document.

Tom Ferrin and UCSF Bioinformatics Program, for two years of funding and a fantastic educational environment.

and

Julia Molla, for helping me navigate the UCSF institution.

Alana Hysert, for being my wife and supporting me in the most patient, wonderful, and kind manner such that I will never be able to fully repay.

Probing Integrin Specificity in regards to Clustering Dynamics on Soft and Stiff Matrices

by

Ryan Gile

Abstract

Integrins are key sensory molecules that transduce chemical and physical cues from the extracellular matrix (ECM) to initiate biochemical signaling and cytoskeletal remodeling to regulate cell behavior and tissue structure. These transmembrane cell-ECM receptors occur as distinct types and drive different cell and tissue level behaviors and consequently also contribute non uniformly to their pathologies. To act integrins cluster in the plasma membrane and recruit scaffolding and signaling molecules required for the mechanical and biochemical functions performed by adhesion-plaques. Regulation of integrin clustering by the material properties of the ECM has been suggested to be a fundamental processes employed by cells to sense and respond to their mechanical environment. However, the molecular mechanisms that drive clustering in response to interaction with the ECM remain unclear. Recent studies have demonstrated a direct link between integrin clustering, increased matrix stiffness, and breast cancer. Additionally data from primary breast cancers suggests α_5-integrin drives invasion while α_2-integrin acts as a tumor suppressor. α_5-integrin is known to have special mechanical properties but recent work on integrin recycling suggests its dynamics may be very different as well. This study employs the high resolution imaging technique of fluorescence recovery after

photobleaching (FRAP) to measure and compare the clustering dynamics of α_5-integrin and α_2-integrin in the non malignant mammary epithelial cell line MCF10A cultured on polyacrylamide gels mechanically tuned to match the compliances exhibited by healthy and pathologic breast tissue.

Table of Contents

Introduction

Tissues are self organizing systems generated by the social behavior of billions of cells interacting locally with each other and the extracellular matrix (ECM). Traditionally soluble factors secreted by cells such as growth factors, hormones and cytokines have been viewed as the sole directives controlling morphogenesis and tissue homeostasis [1]. However, the perceived supremacy of these biochemical cues is waning as a more comprehensive model of tissue development emphasizing the biochemical cues and mechanical forces exerted and experienced by cells and percolated through the ECM is becoming apparent.

Force In Tissues

Cells in tissues are subject to a barrage of forces that include compressive, tensile, fluid shear stress, and hydrostatic pressure, each of which are essential to the shaping, development, and maintenance of the tissue. Throughout morphogenesis cells must exert force to push and pull on each other and the ECM when navigating towards their final position within the nascent tissue. But recent work has shown that mechanical deformations associated with these movements also actively participate in the signaling cascades regulating developmental gene expression [2]. Force interactions also influence embryonic lung branching morphogenesis, guide angiogenesis, and usher germ band extension [44-46]. Once developed long term viability of tissues is predicated upon their ability to maintain structure and function in the face of impugning external forces.

Indeed an essential quality of tissues is the ability to modulate their mechanical strength to withstand/match the forces encountered [3]. In compliant arteries vessel wall thickness is regulated by blood pressure to maintain constant force per unit area and ensure wall integrity. Similarly, rigid structures like bone respond to prolonged changes in mechanical loading by adapting bone density to meet demand. These observations highlight the reactive control tissues exert over their material properties in order to maintain tissue structure and homeostasis [4].

Material Properties of the Extracellular Matrix

The material properties of a tissue emerge from the mechanical interactions of its myriad cells with the ECM [47]. The ECM is the principal extracellular component of all tissues and organs. It provides both the scaffold providing physical support to cells and also regulates intercellular biochemical and biomechanical signaling and plays a role in a number of cellular processes including adhesion, migration, apoptosis, proliferation, and differentiation. The molecular components of the ECM include collagens, elastins, proteoglycans, hyaluronic acid, fibronectin, and laminin. At the molecular level the ECM is capable of binding, integrating, and controlling the presentation of growth factors and other ligands to cells [39]. The organization of the ECM is not static, but is a dynamic structure with varying composition and distribution between different tissues and during the stages of development. Cells constantly pull on the surrounding ECM and in response modify their elastic properties via changes in

actomyosin contractility and cytoskeletal organization tuning themselves to the perceived stiffness of the microenvironment. Concurrently, the ECM is being actively remodeled both in composition and structure due to changes in cellular tension. This interplay between the biophysical properties of the cell and ECM establishes a dynamic, mechanical reciprocity between the cell and the ECM in which the cell's ability to exert contractile stresses against the extracellular environment balances the elastic resistance of the ECM to that deformation [5]. This force balance is a requirement for normal cell function as evidenced by observation that tissue specific cells perform better in ECMs with mechanical properties analogous to their native tissues [6]. Importantly, regulation of the cell-ECM interaction controls tissues homeostasis while its disruption causes loss of tissue architecture and is critical to breast cancer development. For example, mammary epithelial cells (MECs) naturally form hollow acinar structures when grown in soft ECMs of similar stiffness to the normal mammary gland, but create aberrant lumen filled acini with tumor like transcriptional profiles when raised in stiff ECMs of compliance analogous to tumor tissue [7]. Far more is known about the details concerning biochemical regulation of cell behavior and tissue outcomes than the relatively unexplored biomechanical principles also at work and suggested to be dominant. It is therefore important and fundamental to the understanding of tissue homeostasis and pathology to identify the molecular mechanisms by which cells sense and react to the mechanical properties of the ECM.

Mechanotransduction

Insights into how cells sense ECM rigidity come from the study of mechanotransduction, the blanket term for processes used by cells to translate external mechanical forces into biochemical signals. The most well characterized examples of mechanotransduction involve force induced changes to protein conformations. For example, the opening of stretch-activated ion channels within the cell membrane is a result of conformational changes caused by interstitial pressure and membrane deformation and leads to increased intracellular calcium levels [9]. Additionally, changes in cell contractility have been shown necessary to elicit downstream signaling in response to growth factor and G protein-linked receptor stimulation [10]. Indeed, work in mechanotransduction involving the cell-ECM interface is underway and has illuminated a possible mechanical network of proteins and molecules capable of directly linking the ECM with the cell nucleus and site of gene expression [10]. The chief signaling and force sensitive elements in this linkage are the focal adhesion-plaques found at the cell-ECM interface and formed by clusters of transmembrane ECM receptors known as integrins.

Integrins

Integrins have emerged as key sensory molecules that transduce chemical and physical cues from the ECM to initiate biochemical signaling and cytoskeletal remodeling to regulate cell behavior. Individually integrins accomplish little as they lack enzymatic activity, instead they cluster into

4

adhesion plaques to enlist signaling molecules, but the molecular mechanisms

that drive clustering in response to interaction with the ECM remain unclear [12].

Integrins are heterodimeric transmembrane receptors built of non-

covalently associated alpha and beta subunits, with promiscuous binding

partners and differential tissue distributions [13]. Structurally each subunit

contains a large extracellular domain containing a head supported by a series of

flexible linkers, a membrane spanning helix, and a short cytoplasmic tail [14].

The head contains sites for ECM ligand binding and subunit association while the

tail houses the interface for cytoskeletal and adhesion-plaque proteins. The

ability of integrins to bind either extracellular or intracellular ligands is influenced

by its conformational state, which in turn dictates clustering ability. Two major

forms have been identified, an "active" and an "inactive" state. The active state is

characterized by increased affinity for both ECM and cytoplasmic ligands as a

result of integrin elongation by straightening of the flexible linkers causing

enhanced presentation of both head and tail interaction sites. In the inactive

conformation bending of the flexible linkers brings the head near the plasma

membrane and decreases cytoplasmic tail separation, significantly hindering both

extracellular and intracellular interaction sites. Binding of either ECM ligand or

intracellular ligand induces the active conformation and is highly cooperative [15].

Importantly, integrins are capable of bi-directional signaling by propagating

cues across the cell membrane from the inside-out or from the outside-in [16,17].

Inside-out signaling occurs, for example, when binding of talin and kindlin to the

cytoplasmic tails of integrin dimers induces/stabilizes the active state thus

increasing ECM ligand affinity. Outside-in signaling happens when integrin-ECM ligand interactions induces/stabilizes the active form resulting in conformational changes in the integrin transmembrane and cytoplasmic domains that are linked to downstream signaling [14]. Following activation and engagement with ligands, integrins cluster and recruit to the cytoplasmic face of the plasma membrane scaffolding and signaling molecules required for the mechanical biochemical functions associated with integrin based adhesion-plaques.

ECM Rigidity Regulates Integrin Clustering

Evidence that integrins are aware of the physical and chemical properties of the ECM is demonstrated by the influence these properties have on integrin adhesion complex assembly. For example, the number, size, and distribution of integrin complexes in the cell membrane is determined by the density of matrix ligands and their affinity for the integrin receptor [18-21]. In particular integrin clustering is incredibly cognizant of ligand spacing as the ability to assemble large focal adhesion like clusters can be turned on or off by changing the average ligand spacing by nanometer levels [18,20]. Integrin function is also tunable by matrix compliance as rigid matrices encourage large focal adhesion maturation whereas soft substrates give rise to small nascent complexes [7]. Because integrin clustering influences adhesion assembly and the subsequent signaling that dictates cellular behavior, the responsiveness of clustering to the material properties of the ECM represents an essential tool cells may use to sense and respond to their mechanical environment. Improper sensing by

integrins and altered matrix properties both individually and together can cause the disruption of this sensory circuit whose misregulation is implicated in many diseases including cancer.

Integrins in Cancer

Indeed, recent work using mouse models demonstrated imposed ECM stiffening in an oncogene-initiated epithelium promoted focal adhesions, enhanced signaling, and induced invasion. And in the premalignant epithelium inhibition of integrin signaling repressed invasion while forced integrin clustering promoted focal adhesions and induced invasion into a stiffened ECM [24]. Thus ECM stiffness as perceived by integrins regulated the transition from tissue homeostasis to malignancy.

Integrin Specificity

However, not all integrins are equally implicated in the drive towards malignancy caused by ECM stiffening. Nonmalignant mammary epithelial cells express a suite of different integrins including the 'differentiation-associated' laminin/collagen receptor α_2-integrin but not regularly the 'invasion and growth-linked' fibronectin receptor α_5-integrin. However, expression levels of α_5-integrin increase during wound healing and in tumors. Indeed, α_5-integrin has been shown to drive invasion while α_2-integrin can act as a tumor suppressor. Supportingly, data show that primary human breast tumors frequently present a reduction in expression levels for α_2-integrin but reveal increased expression of

α_5-integrin [25]. Additionally, ECM stiffness-dependent lineage studies using human mesenchymal stem cells indicate cellular fate is ECM ligand specific. Compliant collagen based ECMs promoted neurogenesis whereas cells cultured on similarly compliant fibronectin based ECMs underwent adipogenesis[17]. These results collectively support the assertion integrin specificity, in particular the presence and activity of α_5-integrin vs. α_2-integrin, has dramatic and important consequences at the cell and tissue level ultimately determining the difference between healthy and pathologic states.

What drives these integrin specific phenotypic outcomes? I suggest there are inherent differences either in the signaling or in the force responsiveness/ mechanotransduction of $\alpha_5\beta_1$ versus $\alpha_2\beta_1$. Their is not conclusive evidence that differences in signaling drive specificity. There is evidence the difference lies in the nature of their mechanical interactions with the ECM. Experiments have shown that $\alpha_5\beta_1$–fibronectin links form catch bonds that strengthen under force[22] and as a result high matrix forces are primarily supported by clustered $\alpha_5\beta_1$ integrins [28]. Furthermore, the strength of integrin binding to fibronectin is a requirement for initiating and propagating fibril formation but the ability to achieve sufficient bond strength for assembly is a unique property of $\alpha_5\beta_1$ [42]. Importantly recent work has shown only when $\alpha_5\beta_1$ binds to fibronectin in a high tension state that involves the fibronectin synergy site does it becomes capable of activating FAK and transmitting down stream signals [43]. I hypothesize then that $\alpha_5\beta_1$ is specifically enriched/selected for in tumors such as breast cancer because it exhibits unique force sensing and transducing effects.

Accordingly understanding the molecular mechanisms whereby it is modulated/regulated in cells is critically important. One observation suggests that $\alpha_5\beta_1$ integrin turnover is quite different from other integrins such as $\alpha_v\beta_3$ [48]. There has not been similar work comparing $\alpha_2\beta_1$. Therefore, I intend to study the dynamics of integrins in detail in order to determine the fundamental distinctions between α_5-integrin and α_2-integrin to understand the mechanism by which integrin specificity shapes tissue outcomes. In particular I will focus on how measuring the difference between α_5-integrin and α_2-integrin dynamics on soft and stiff substrates.

FRAP

To probe the difference in integrin dynamics I turn experimentally to one of the best techniques for measuring the internal dynamics of complex structures, fluorescence recovery after photobleaching (FRAP) [27]. FRAP is a high resolution imaging technique that can provides estimates of binding kinetics based on the lateral diffusion of a protein within the plasma membrane. Previous work using FRAP to investigate focal adhesion protein dynamics has successfully determined the relative recruitment rates of individual players, including integrins, into adhesive structures [28]. For effective and validated ECM surrogates I will use polyacrylamide gels tuned over a range of compliances and functionalized with various ECM ligands. Thus I will use FRAP to assess α_5-integrin vs. α_2-integrin clustering dynamics on soft and stiff ECM substrates with the aim of leveraging this information into meaningful insights about the role integrin

specificity plays in sensing ECM compliance and regulating the transition to malignancy.

MATERIALS & METHODS

Reagents:

For preparation of 2D cell substrates, the following ECM proteins were used: Lyophyilized bovine fibronectin (reconstituted in H_2O, Sigma); Vitrogen 100 bovine skin collagen I (Celtrix Laboratories); Matrigel™ tumor derived basement membrane (Collaborative Research).

Cell Culture:

Cell Lines

The spontaneously immortalized non-transformed human mammary epithelial MCF10A cell line[29] was used to answer questions about integrin dynamics in normal breast epithelial biology. The cell line was derived from a patient with a fibrocystic disease and exhibits a phenotype similar to normal mammary epithelium [29]. For example, it is anchorage-dependent, relies on growth factors and hormones for proliferation and survival, lacks tumorgenicity when injected into nude mice, and undergoes morphogenesis to form spherical acini when grown within a compliant 3D recombinant basement membrane hydrogel *in vitro*. These acini resemble normal mammary lobular epithelium *in vivo* and are characterized by apical-basal polarity, stable cell-cell junctions, basal deposition of basement membrane proteins, and apoptosis-induced hollow lumens.

The MCF10A cell line is susceptible to phenotypic drift during long term cell culture. Careful attention must be paid to the morphology of this cell line during routine cell culture. The passage number with which we used this mammary epithelial cell (MEC) line in experiments was therefore limited to below passage 30.

2D Monolayer Cultures

MCF10A cells were grown as monolayers on polystyrene dishes and were maintained in standard tissue culture incubators at 37°C and 5% CO_2. The growth medium, composed of DMEM:F12 supplemented with 5% Donor Horse Serum, 20 ng/mL EGF, 10 µg/mL insulin, 0.5 µg/mL hydrocortisone, 100 ng/mL cholera toxin, and 1% (v/v) Penicillin/Streptomycin (100 I.U./mL Penicillin, 100µg/mL Streptomycin), was changed every two to three days. When cultures reached approximately 75% confluency, cells were trypsinized with 0.25% Trypsin-EDTA and resuspended in DMEM:F12 supplemented with 20% donor horse serum.

Functionalized Glass Substrates

Glass coverslides were functionalized with ECM proteins such as collagen, laminin, and fibronectin to create 2D substrates for the culture of cells *in vitro.* For short term cultures, the ECM was applied to glass coverslips and allowed to dry. Collagen (2.9 mg/ml) was diluted 1:50 with 30% ethanol and the solution was spread over the surface of a sterile glass coverslip and allowed to air dry in a tissue culture hood. Cells were then directly seeded on the collagen

surface. Fibronectin was diluted in PBS to produce a 10ug/ml solution that was

spread over the surface of a sterile glass coverslip and incubated for 30-45

minutes at room temperature. After incubation the remaining solution was

aspirated and the coverslides were rinsed with PBS. Cells were then directly

seeded on the fibronectin surface. Matrigel was diluted with a chilled buffer

(0.1M HEPES and 0.1M NaCl pH8) to create a 100ug/ml solution that was

spread over a sterile glass coverslip and stored in a 4C refrigerator for 1-2 days.

After refridgeration the remaining solution was aspirated and rinsed 2-3 with

PBS. Cell were then directly seeded on the Matrigel surface.

Functionalized Polyacrylamide Gels

Polyacrylamide gels were functionalized with ECM proteins to create 2D

substrates for the culture of MECs. I chose polyacrylamide because it is an

excellent material for the culture of MECs since it is biocompatible, non-toxic,

resistant to non-specific absorption of proteins, and optically clear for microscopy

applications. Moreover, mechanical stiffness of polyacrylamide substrates can

be precisely modulated by adjusting the concentrations of acrylamide or bis-

acrylamide prior to polymerization [30].

As illustrated in Figure M1 the procedure I used to prepare the

polyacrylamide cell substrates is as described. First, coverslips were chemically

activated to permit the covalent attachment of the polyacrylamide gel. This was

achieved by placing glass coverslips (#1) in a Petri dish and incubating with 0.2M

HCl for 1 hour. The coverslips were then washed three times in ddH$_2$O for 5

minutes and incubated with 0.1M NaOH for 10 minutes. Coverslips were then

washed three times in ddH$_2$O for 5 minutes and then incubated with 0.5% (v/v)

aminopropyltrimethoxysilane (in ddH$_2$O) for 30 minutes. Coverslips were next

washed three times for at least 10 minutes each in ddH$_2$O, incubated with 0.35%

(v/v) glutaraldehyde for 1 hour, and rinsed thoroughly three times in ddH$_2$O for 10

minutes. All of the above manipulations were performed at room temperature on

an orbital shaker. Finally, the activated coverslips were allowed to dry overnight

at room temperature.

Polyacrylamide gel solutions were prepared using acrylamide (40% w/v

solution; Bio-Rad Laboratories, Hercules, CA), N, N-methylene-bis-acrylamide

(2% w/v solution; Bio-Rad Laboratories, Hercules, CA), N,N,N',N'-

Tetramethylethylenediamine (TEMED; Bio-Rad Laboratories, Hercules, CA),

ammonium persulfate, and the bifunctional crosslinker N-succinimidyl ester of

acrylamidohexanoic acid (N6 crosslinker). The N6 crosslinker was synthesized

in-house using the method described by Pless and colleagues [31]. The N6

crosslinker covalently binds to the acrylamide and has an N-succinimidyl ester

that is displaced by a primary amine during the functionalization step to link the

amine-containing ligand to the polyacrylamide gel.

Polyacrylamide gel solutions were prepared following the recipes in Table

2.3 (Note: All values stated below are for 1mL final polyacrylamide solution.)

The polyacrylamide solutions were de-gassed using a vacuum flask for at least

30 minutes. 5.6mg of N6 crosslinker was weighed out and combined with 70uL

of 200 proof ethanol and 80uL of ddH$_2$O. The crosslinker solution was vortexed

and then briefly sonicated (in a sonicating water bath, average peak power = 45W) until dissolved. After de-gassing, the N6 crosslinker solution was added to the polyacrylamide solution. A 1/100 volume of 5% ammonium persulfate was added to the mix immediately prior to gel dispensing. A predetermined volume of solution was then pipetted onto an activated coverslip (25ul for an 18mm coverslip and 200uL for a 50mm coverslip), and the gel was sandwiched by a Rain-x coated coverslip of the same size.   The gels were incubated at room temperature until polymerization was complete (25-45 minutes), which was visually detected by whether or not there was an initial retraction of the gel from the edge of the coverslip. After the gels had fully polymerized, the top coverslip was carefully removed from the gels using a razorblade. Each gel was then rinsed with ice cold ddH$_2$O, and incubated with a rBM (140µg/mL Matrigel and 5mM EDTA, pH 8.0 in ice cold 50mM HEPES, pH 8.0) or fibronectin solution (100 µg/mL bovine fibronectin in 50mM HEPES buffer, pH 8.0), or collagen solution (50 µg/mL collagen in sterile PBS) for 2 hours on ice. The protein-coated gels were then rinsed in ice cold ddH$_2$O and the unreacted N6 crosslinker was blocked by incubation with 1/100 volume of ethanolamine in 50mM HEPES buffer, pH 8.0 for 30 minutes on ice. Prepared gels were then rinsed in PBS, stored overnight in sterile PBS at 4°C (See Figure 2.2 for schemata of preparation). The following day, the gels were rinsed extensively in sterile PBS, irradiated for 30 minutes under an anti-microbial UV lamp, and plated with a single cell suspension in growth media. For all experiments cells were grown in

their respective normal growth medium with addition of 1% (v/v) Penicillin/

Streptomycin as an anti-microbial agent.
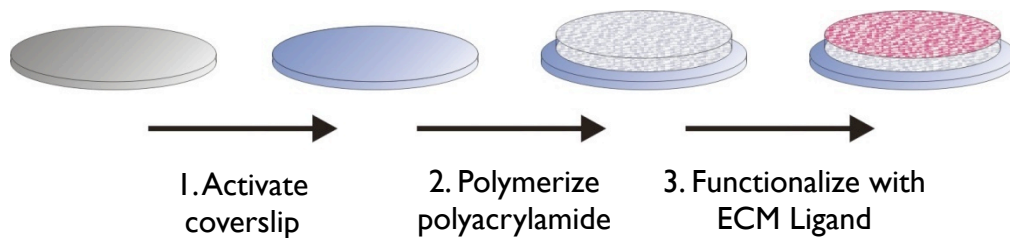
Figure M1. Preparatory steps of functionalized polyacrylamide gels.
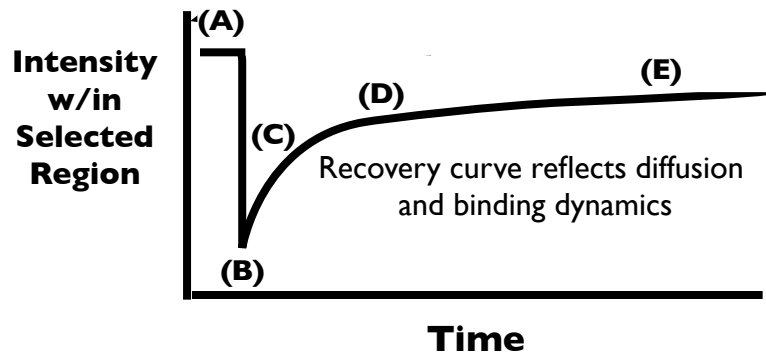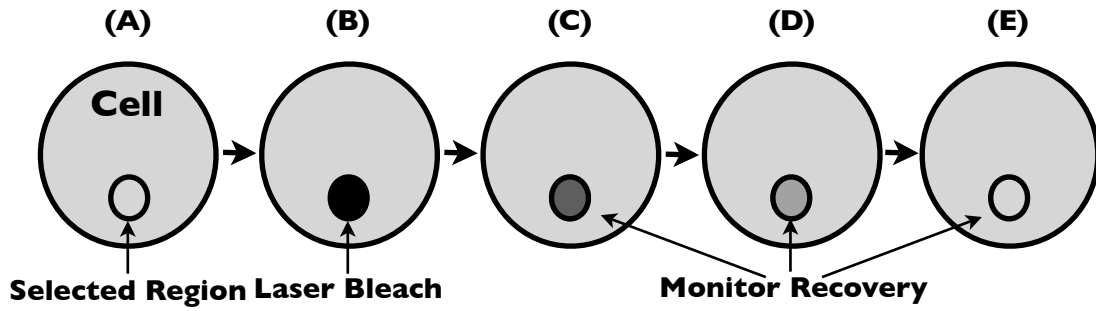
Functionalized polyacrylamide gels were prepared by the following steps: 1.) activation of the coverslips by silanization, 2.) preparation and polymerization of crosslinker/ polyacrylamide solution, 3.) functionalization of polyacrylamide gels through conjugation cross-linking with extracellular matrix.

FRAP

Fluorescence recovery after photobleaching (FRAP) is a quantitative technique that provides estimates of *in vivo* binding dynamics based on the motions of fluorescently tagged molecules repopulating a bleached region within live cells [32].

FRAP relies upon availability of an intracellular fluorescently tagged protein to be bleached, a laser for bleaching fluorophore, a timelapse microscope to observe the replenishment of the bleached region, and using a mathematics program to perform the curve fitting necessary for obtaining quantitative estimates of binding parameters. Briefly my FRAP experiments were carried as follows (**Figure Frap M2)**: 1) A region of interest containing the fluorescently tagged protein was chosen. 2) The selected region of interest was monitored to establish a prebleach intensity providing a baseline for comparison of relative rates of recovery. 3) The region was then bleached using a laser. 4) The time evolution of fluorescence recovery was recorded until recovery was complete or reached a plateau. Successful experiments relied upon an accurate knowledge of pre-bleach intensity, quick and thorough bleaching, and rapid imaging of the post bleach recovery. Optimizations for these steps and additional considerations were as described below.

(A)   **(B)**   **(C)**   **(D)**   **(E)**

Cell

Selected Region   Laser Bleach   Monitor Recovery

Intensity w/in Selected Region

(A)

(B)

(C)

(D)

(E)

Recovery curve reflects diffusion and binding dynamics

Time

Figure M2. FRAP Experiment Diagram. *Top: Cartoon of bleached region in cell with time evolution of its fluorescent recovery with letters designating specific time points. Bottom: Fictional intensity data from fluorescent recovery process as depicted in the cartoon cell with letters designating same time points.*

Fluorophore, Microscope and Laser Choice

To provide meaningful data a FRAP experiment required a tagged protein that was not easily photobleached during the prebleach or recovery phase of the experiment, but was amenable to rapid laser induced bleaching.

Because in FRAP the fluorophore commonly employed is in the form of either a stably expressing or transiently transfected GFP-fusion protein I chose this fluorophore for my experiments. For a baseline comparison, I chose MCF10A cells expressing unconjugated GFP [34]. I chose GFP because of its resistance to photobleaching at low intensity (the pre and post bleaching image acquisition times) and it is readily and irreversibly photobleached at high illumination (the bleaching phase) [35].

Optimally for FRAP experiments the bleach spot should consist of a simple shape such as a rectangle or circle to simplify analysis [33,36-38]. By contrast complex geometries require time consuming and computationally expensive numerical solutions to differential equations. Ideally the minimal size of the bleached region should be large enough to contain enough pixels such that its average intensity remains uniform [34]. Based upon these parameters the size of the bleach spot can be used to infer information about the underlying dynamics. If the recovery is diffusion coupled then the spot size will effect the recovery rate. The number of prebleach images are therefore chosen to maintain an approximately constant intensity level within the region of interest. Ideally postbleach imaging should begin immediately after the bleach period, sample frequently, and remain until the recovery is complete or has plateaued.

Fast and slow regimes are indicated by the presence of multiple plateaus. Sample rates are adjusted according to the presence or absence of plateaus. Laser intensity pre and post bleach acquisition phases is maintained constant at a level set to sufficiently resolve the fluorescent proteins while minimizing any bleaching. The laser power during the intentional bleaching phase is adjusted to reduce the intensity within bleach region by at least 50% which ensures sufficient recovery data for accurate fitting analysis. The duration of the bleach is set to be as short as possible in order to minimize bleaching of the replenishing fluorescent population and to approximately meet the instantaneous bleach assumption imposed by many models.

Data Acquisition

Individual photobleaching experiments were performed in a region where multiple focal adhesions were present. For each bleached adhesion the intensity of a nearby control adhesion as well as the background intensity (region outside of cell) were gathered.

Recovery Curve Creation

As the first step in this process I measured the intensity within the bleach spot and the nearby control adhesion as a function of time. Typically, I discarded spatial information at this point, and the average of all pixels within the bleach spot was calculated. These intensities were then plotted as a function of time to generate the raw FRAP curve **(Figure M3A)**. Important points on a recovery

curve include the average prebleach intensity, F_i, the intensity immediately after bleaching, F_o, and the asymptote of the recovery, F_∞.

Using the raw curve I then subtracted the average background intensity from the average intensity within the bleach spot and the control. Background was measured as the average intensity in a region of the image that contains no cell. This background-subtracted average bleach spot intensity was then normalized to construct the normalized recovery curve.

$$R_{norm}(t) = \frac{F_{bleach}(t) - F_{bgd}(t)}{F_{ctr}(t) - F_{bgd}(t)}$$

Eq. (1)

Finally, this curve was converted to the fractional fluorescence recovery curve by setting its zero point to F_o *(Figure M3B)*.

$$R_{frac}(t) = \frac{R_{norm}(t) - F_0}{1 - F_0}$$

Eq. (2)

Raw Data

Intensity w/in Bleached Region

F_i

F_∞

F_∞

F_o

F_o

0

Time

Fractional Fluorescence Recovery

Fractional Recovery (%) w/in Bleached Region

100

I_f

F_∞

F_∞

$F_\infty {}_{1/2}$

$F_\infty {}_{1/2}$

M_f

0

$t_{\infty {}_{1/2}}$

Time

Figure M3. FRAP Recovery Data A) Raw Data. *Fictional intensity curve representing unmodified FRAP data, with important values indicated.* ***B) Fractional Recovery Data.*** *Fictional Raw data transformed to a Fractional Recovery curve, the final form often necessary for application of different math models.*

Data Analysis

Three kinetic parameters of a protein, the mobile fraction, M_f, the half maximal recovery time, $t_{1/2}$, and the association constant, k_{on}, were gleaned from information in the fractional fluorescence recovery curve. The mobile fraction was interpreted as the fraction of fluorescent proteins that diffused into the bleached region during the timecourse of the experiment. I concluded that mobile fractions less than 100% designated a subpopulation that were not freely diffusing and must have been impeded by either binding events or steric hinderance.

$$M_f = \frac{(F_\infty - F_0)}{(F_i - F_0)}$$

Eq. (3)

The value of the half maximal fluorescence recovery time, $t_{1/2}$, is defined to be the time it takes for the fluorescence intensity to recover half its asymptotic value, $F_{\infty 1/2}$ [27].

$$F_{\infty \frac{1}{2}} = \frac{(F_\infty - F_0)}{2}$$

Eq. (4)

It is related to the diffusivity of the protein and thus also reflects binding events [27,32]. In my thesis photobleaching of integrin adhesion proteins was modeled

with a simple exponential decay curve, **Eq. (5)**, so that binding parameters could be determined [27].

$$F(t) = M_f \cdot \left(1 - e^{-k_{on} \cdot t}\right)$$

Eq. (5)

Where k_{on} is the association constant for the protein associating with the adhesion.   The association rate constant was related to the half maximal recovery time using $t_{1/2}$ and $F_{\infty 1/2}$ to deduce k_{on} according to **Eq. (6).**

$$k_{on} = \frac{\ln(2)}{t_{\frac{1}{2}}}$$

Eq. (6)

Eq (5) and **Eq. (6)** apply to many proteins that undergoes reversible association within the focal adhesion [27].

Microscope and Laser Settings

FRAP experiments were carried out on a Zeiss LSM510 Meta confocal microscope. The Objective was a Plan-Apochromat 63x/1.40 Oil DIC M27. Excitation laser for GFP FRAP was the LSM510 Laser Module 30mW Argon 488nm with MBS: HFT 488/543 beam splitter and a BP 505-570 filter. Excitation laser for mCherry FRAP was the LSM510 Laser Module 1.2mW HeNe 543nm with MBS: HFT 488/543 beam splitter, DBS2: NFT 545 beam splitter, and a LP 560 filter. Experiments were performed in CO2 Cell Culture Buffer at 37C.

Microscope Settings:

Parameter	Value
Imaging Laser Power Output/Transmission	40% / 12%
Bleaching Laser Power Output/Transmission	40% / 100%
Objective	Plan-Apochromat 63x/ 1.40 Oil DIC M27
Pixel Depth	8 bit
Frame Size (Pixel)	512 x 512
Frame Size (μm)	35.7 x 35.7
Scaling	0.07μm x 0.07μm
Scan Speed	8
Pixel Time	1.61 μs
Scan Time	1.57 s
Bleach region shape	circular
Bleach spot size	~7-10 μm^2
Bleach scan speed	25.61 μs
Bleach iterations	15
Number of pre bleach images	3
Number of frames	50
Frame interval	250msec

Table I. Microscope and Laser Settings.

Elastic Modulus (Pa)	Desired % Acrylamide	Desired % Bisacrylamide	40% Acrylamide (uL)	2% BisAcrylamide (uL)	10x PBS (uL)	ddH2O (uL)	1/100 dilution of TEMED (uL)	1% PPS (uL)	Total volume (uL)
600	7.5	0.01	93.75	2.5	50	253.75	50	50	500
6000	7.5	0.07	93.75	17.5	50	238.75	50	50	500
13800	7.5	0.15	93.75	37.5	50	218.75	50	50	500
22000	7.5	0.25	93.75	62.5	50	193.75	50	50	500

Table II. Reagent Volumes for preparation of Polyacrylamide Gels.

CHAPTER 1

Introduction

Cells in tissues inhabit a dynamic structural protein network, the extracellular matrix (ECM), which they secrete into the intercellular space, and constantly remodify. In this environment they encounter numerous biochemical and physical cues that guide their behavior.

The extracellular matrix (ECM) directs developmental programs such as cell and branching morphology of various epithelium including lung, salivary gland, and breast tissue. As such clarifying the molecular mechanisms by which ECM elicits these effects has been the subject of much study.

Integrins are the prime mechanical and chemical linkage between cells and the ECM. Integrins are heterodimeric transmembrane receptors built of non-covalently associated alpha and beta subunits. Structurally each subunit contains a large extracellular domain containing a head with ECM ligand binding and subunit association properties, connected by flexible linkers to a short cytoplasmic tail where cytoskeletal and adhesion plaque proteins may bind [14]. They have two important conformations known as the "active" state distinguished by high affinity for both ECM and cytoplasmic ligands, as well as the "inactive state" branded by low ligand affinity. Importantly, intracellular and extracellular ligand binding is highly cooperative as each serves to activate the integrin.

It is this cooperative activation that allows integrins to carry out bidirectional signaling across the plasma membrane known as "inside-out" and "outside-in" signaling. Inside-out signaling occurs when intracellular ligands bind

the integrin cytoplasmic tails and induces/stabilizes the active state thus increasing ECM ligand affinity. Outside-in signaling happens when integrin-ECM ligand interactions induces/stabilizes the active form resulting in conformational changes in the integrin transmembrane and cytoplasmic domains that are linked to downstream signaling [14]. Post activation and engagement with ligands integrins laterally cluster and recruit scaffolding and signaling molecules required for the mechanical biochemical functions performed by integrin based adhesion-plaques.

Regulation of integrin clustering is crucial to maintenance of normal cellular function. One important regulator of integrin conduct is the physical and chemical properties of the ECM which influences integrin adhesion complex assembly. For example, the number, size, and distribution of integrin complexes is determined by the density of matrix ligands and their affinity for the integrin receptor [18-21]. Integrin function is sensitive to matrix compliance with stiff matrices exhibiting large focal adhesions, in contrast soft substrates give rise to small dot-like nascent focal complexes [7]. Because integrin clustering controls adhesion assembly and the consequent signaling that determines cellular behavior, the responsiveness of clustering to the material properties of the ECM provides an essential tool cells may exploit to sense and respond to their mechanical environment. Disruption of this sensory circuit by faulty integrins or increased matrix stiffness is implicated in many diseases including breast cancer.

One biological mechanism that increasingly is being recognized as having important control over integrin-mediated activities is the trafficking of the integrins themselves. This process consists of complex intracellular internalization and recycling pathways [51]. Recent evidence suggest a role for integrin trafficking during the invasive migration of cancer cells through 3D microenvironments [53]. Provocatively integrin endocytosis and recycling has been show to influence the deposition and remodeling of fibronectin [52]. Other trafficking studies have shown that $\alpha_5\beta_1$ integrin turnover is quite different from other integrins such as $\alpha_v\beta_3$. Together this suggest integrin turnover dynamics are important for many processes, may be different between integrins, and may be altered on stiffer substrates. Thus it is essential to measure integrin dynamics in different contexts in order to illuminate the details of their regulation.

As such techniques to quantify integrin dynamics have recently gained attention. One powerful approach for measuring integrin dynamics within the complex structure of focal adhesions is the high resolution imaging method of fluorescence recovery after photobleaching (FRAP). FRAP is a quantitative technique that provides estimates of *in vivo* binding dynamics based on the motions of fluorescently tagged molecules repopulating a bleached region within live cells [32]. Binding estimates are obtained by fitting the fluorescence intensity recovery curve to a mathematical model of the binding interactions. In many cell types such as fibroblasts and osteosarcomas FRAP has been used to monitor the dynamics of diverse proteins including integrins within focal adhesions. However, it has yet to be employed in a mammary epithelial cell (MEC) line.

My interest in the dynamics of integrins is due to their contribution to normal breast epithelial biology and therefore I chose to use the spontaneously immortalized non-transformed human mammary epithelial MCF10A cell line[29] for these FRAP studies. The cell line was derived from a patient with a fibrocystic disease and exhibits a phenotype similar to normal mammary epithelium [29]. For example, it is anchorage-dependent, relies on growth factors and hormones for proliferation and survival, lacks tumorigenicity when injected into nude mice, and undergoes morphogenesis to form spherical acini when grown within a compliant 3D recombinant basement membrane hydrogel *in vitro*. These acini resemble normal mammary lobular epithelium *in vivo* and are characterized by apical-basal polarity, stable cell-cell junctions, basal deposition of basement membrane proteins, and apoptosis-induced hollow lumens.

As my first step towards understanding the role of integrin dynamics in MEC behavior I constructed a FRAP system to quantify those dynamics. I chose to do preliminary studies measuring integrin dynamics indirectly by using the generic focal adhesion marker Paxillin [49] whose dynamics within adhesions have been reported in the literature [50] and thus provided a means of assessing the success of my experimental approach. Paxillin is an adapter protein with roles in linking scaffolding and signaling in the adhesion plaque. LIM domains within the C-terminal region of Paxillin target it to focal adhesions where they are suspected to directly associate with the cytoplasmic tails of β integrins [49]. Rich in interaction sites, its N-terminal region facilitates binding to other important adhesion signaling molecules such as Src and FAK, as well as scaffolding

proteins like vinculin [49]. The direct association between Paxillin and integrin β

tails make it an ideal marker for both $\alpha_2\beta_1$ and $\alpha_5\beta_1$.

To do FRAP studies on Paxillin requires a fluorescent tag. Ideally, GFP is

used due its resistance to bleaching by laser at normal imaging levels and its

rapid bleaching by high intensity laser bombardment. However, I chose to use

the more photostable mCherry fluorophore to imagine paxillin because prior work

in our lab demonstrated its good incorporation into focal adhesions.

For the mathematical model of paxillin behavior I chose to neglect

detailing the specific interactions between paxillin and the various adhesion

components and instead lump those complex dynamics into a simple

association/dissociation reaction of paxillin with the adhesion. This model

provides a simple exponential fit, Eq(5)(See Methods), to the FRAP curve which

can be used to determine the paxillin association rate constant, k_{on} , a useful

parameter when comparing the relative dynamics of an adhesion protein across

different scenarios. I also report the half maximal fluorescence recovery time,

$t_{1/2}$, which is defined to be the time it takes for the fluorescence intensity to

recover half its final value and is dependent on the diffusivity of paxillin. The

association rate constant is related to the half maximal fluorescence recovery

time by Eq(6). Finally the last binding estimate I report is the mobile fraction,

which is interpreted as the fraction of fluorescent proteins that diffused into the

bleached region during the timecourse of the experiment Eq(3). Mobile fractions

less than 100% indicate a subpopulation of paxillin molecules that were not freely

diffusing and most likely have been impeded by binding events (Figure 1.1).

Paxillin
association

k_{on}

k_{off}

Paxillin
dissociation

| Actin | Integrin | Paxillin | Talin | ECM ligand |
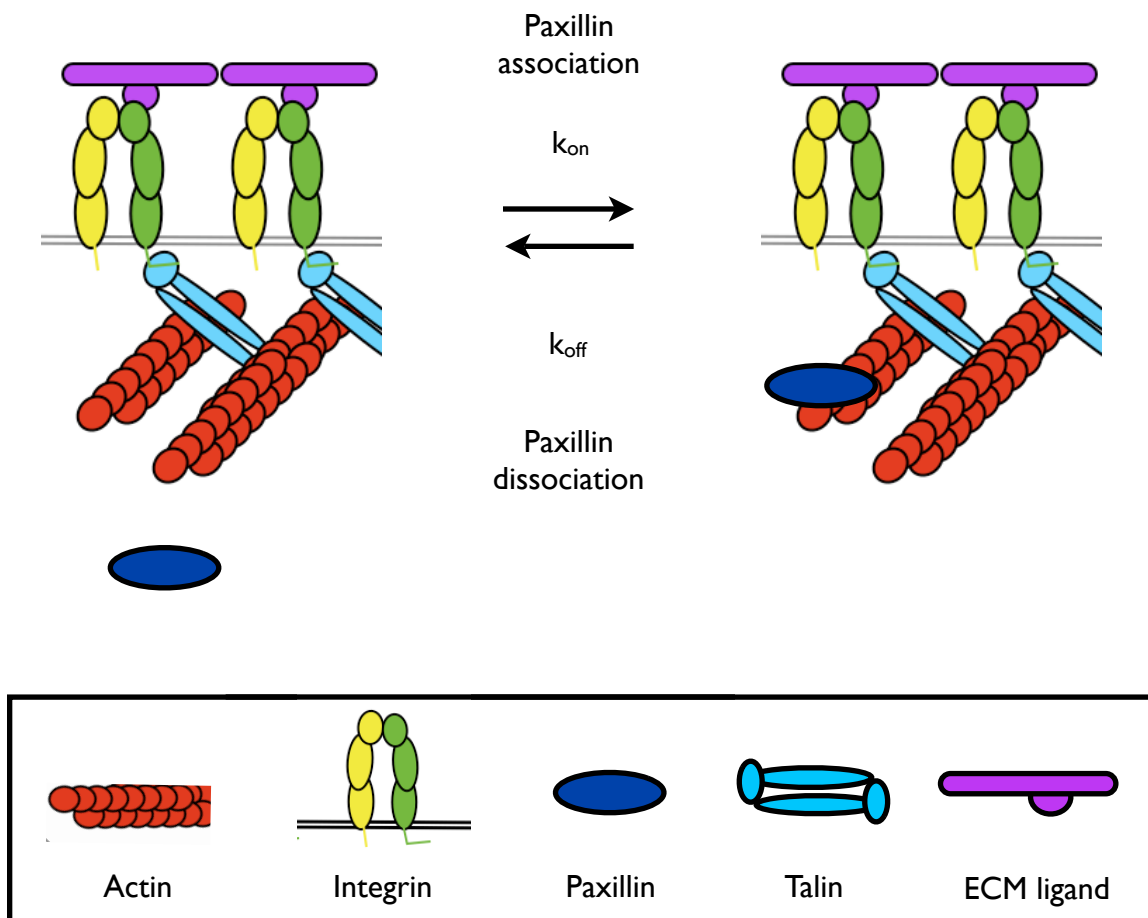
Figure 1.1. Simple Model of Paxillin interaction with focal adhesions. *Paxillin interacts with many players in a focal adhesion, such as actin, integrin, talin, and various other signaling molecules. These details are suppressed in favor of a single association/ dissociation model facilitating simpler mathematical analysis. Adapter with permission from [27].*

Results

I created the mCherry-Paxillin construct for the MCF10A mammary

epithelial cell line. The mCherry-Paxillin MCF10A cells were cultured on tissue

culture plastic with a maximal passage number of 30 and displayed normal

spreading and growth curves for the cell line. Confocal imaging of mCherry-

Paxillin showed good localization to large focal adhesions with high expression

levels.

I successfully functionalized glass coverslips with fibronectin protein. The

mCherry-Paxillin MCF10A cells were seeded on the collagen slides 24 hours

before each FRAP experiment. Cells readily divided and exhibited

phenotypically normal spreading.

For my FRAP experiments using mCherry-Paxillin I optimized microscope

and laser settings for the pre-bleach, bleach, and post-bleach phases (See

Method Microscope and Laser settings for an enumerated list of parameter

settings). For mCherry-Paxillin expressing MCF10A cells on fibronectin

conjugated glass I calculated an Paxillin association rate of 0.069 s^{-1}, a half time

of recovery of 10 s, and a mobile fraction around 57% **(Figure 1.2).**

FRAP of MCF10A mCherry Paxillin on Fibronectin conjugated Glass

$k_{on} = 0.069 \ s^{-1}$

$t_{1/2} = 10 \ s$

Mobile Fraction = 57 %
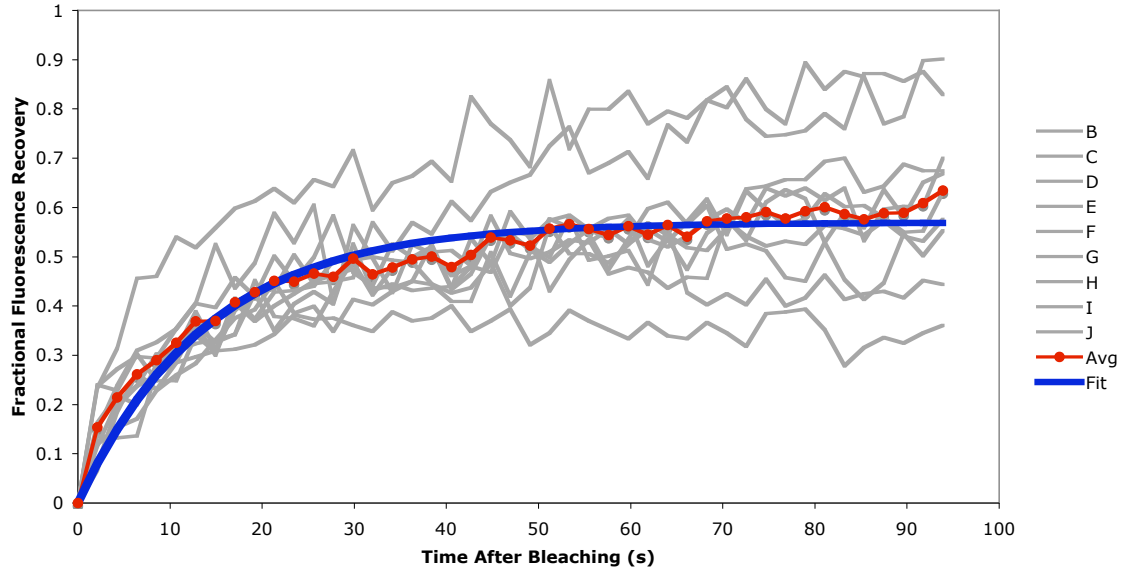
Figure 1.2 **MCF10A mCherry Paxillin Dynamics on Fibronectin coated Glass.** *Grey lines represent FRAP experiments performed on individual adhesions within different cells. Red line is average recovery curve of all experiments. Blue line is the data fit according to the Equation (6) (See Methods). Error bars are +/- standard error.*

Discussion

In NIH3T3 cells expressing YFP-Paxillin cultured on fibronectin conjugated glass previous work using FRAP has determined the association rate constant of paxillin to be 0.063 s^{-1} with a mobile fraction near 70% [50]. This association rate constant deviates from my reported value by ~10%. Thus I conclude the FRAP system is able to accurately quantify the dynamics of a generic focal adhesion protein in a nonmalignant breast cell line on an ECM conjugated substrate of extremely high stiffness.

CHAPTER 2

Introduction

Nonmalignant mammary epithelial cells express on their surface a variety of the different cell-ECM receptors known as integrins. For example, they normally express the collagen receptor α_2-integrin, but they do not normally express the fibronectin receptor α_5-integrin. However, during wound healing and tumors α_5-integrin levels increase. Indeed, α_5-integrin has been shown to drive invasion while α_2-integrin can act as a tumor suppressor. Supportingly, data show that primary human breast tumors frequently present a reduction in expression levels for α_2-integrin but reveal increased expression of α_5-integrin [25]. Additionally, ECM stiffness-dependent lineage studies using human mesenchymal stem cells indicate cellular fate is ECM ligand specific. Compliant collagen based ECMs promoted neurogenesis whereas cells cultured on similarly compliant fibronectin based ECMs underwent adipogenesis[17]. These results collectively support the assertion integrin specificity, in particular the presence and activity of α_5-integrin vs. α_2-integrin, has dramatic and important consequences at the cell and tissue level ultimately linked to regulation of healthy and pathologic states.

What drives these integrin specific phenotypic outcomes? I suggest there are inherent differences either in the signaling or in the force responsiveness/ mechanotransduction of $\alpha_5\beta_1$ versus $\alpha_2\beta_1$. Their is not conclusive evidence that differences in signaling drive specificity. There is evidence the difference lies in the nature of their mechanical interactions with the ECM. Work has shown that

$\alpha_5\beta_1$–fibronectin links form catch bonds that strengthen under force[22] and as a result high matrix forces are primarily supported by clustered $\alpha_5\beta_1$ integrins [28]. Furthermore, the strength of integrin binding to fibronectin is a requirement for initiating and propagating fibril formation but the ability to achieve sufficient bond strength for assembly is a unique property of $\alpha_5\beta_1$ [42]. Importantly recent work has shown only when $\alpha_5\beta_1$ binds to fibronectin in a high tension state that involves the fibronectin synergy site does it become capable of activating FAK and transmitting down stream signals [43]. I hypothesize then that $\alpha_5\beta_1$ is specifically enriched/selected for in tumors such as breast cancer because it exhibits unique force sensing and transducing effects.

To indirectly test this hypothesis I employed the optimized FRAP system for MCF10A mCherry-Paxillin on fibronectin coated glass to measure paxillin dynamics on collagen, and rBM (collagen, laminin) coated glass.

Results

Glass coverslips were successfully functionalized with various ECM. Prior to each FRAP experiment the mCherry-Paxillin MCF10A cells were seeded on the ECM coated slides for 24 hours. Cells readily divided and exhibited phenotypically normal spreading.

For mCherry-Paxillin expressing MCF10A cells on collagen coated glass I report a Paxillin association rate of 0.087 s^{-1}, a half time of recovery of 8 s, and a mobile fraction around 49%. On Matrigel coated glass I determined a Paxillin

association rate of 0.125 s^{-1}, a half time of recovery of 5.5 s, and a similar mobile

fraction around 44%.
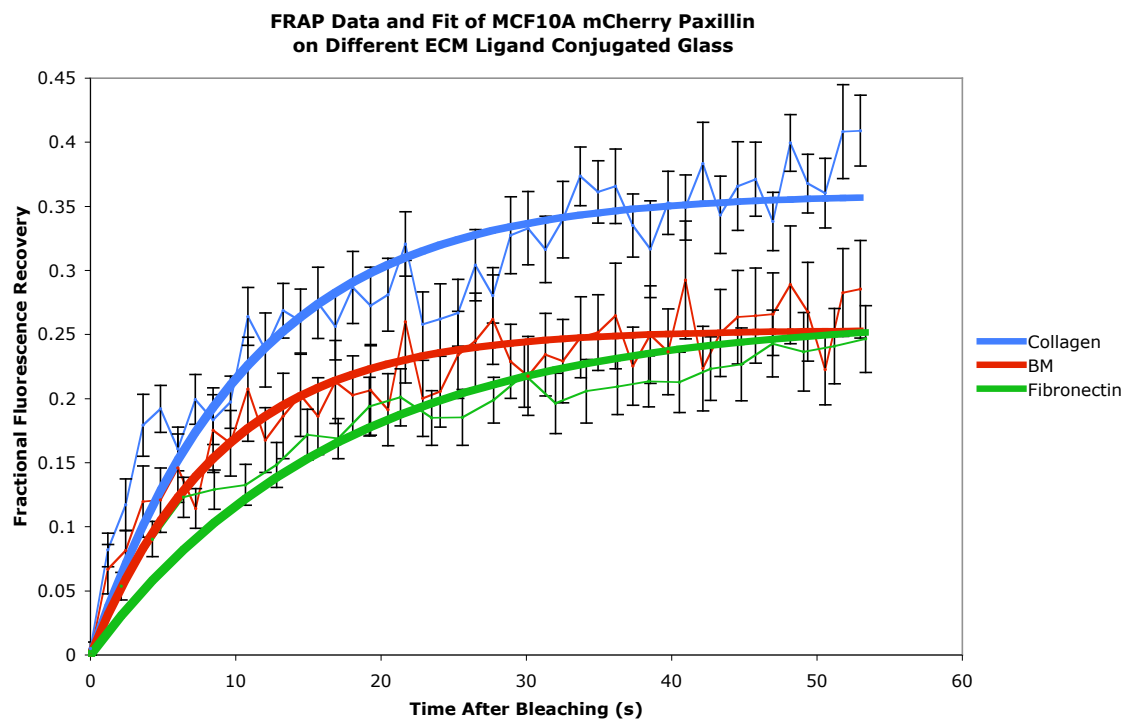
Figure 2.1 MCF10A mCherry Paxillin Dynamics on ECM coated Glass. *Thin lines represent the average recovery curve on individual ligand. Thick lines represent fit for average curve.. Error bars are +/- standard error.*

**MCF10A mCherry Paxillin
Association Rate vs ECM ligand**
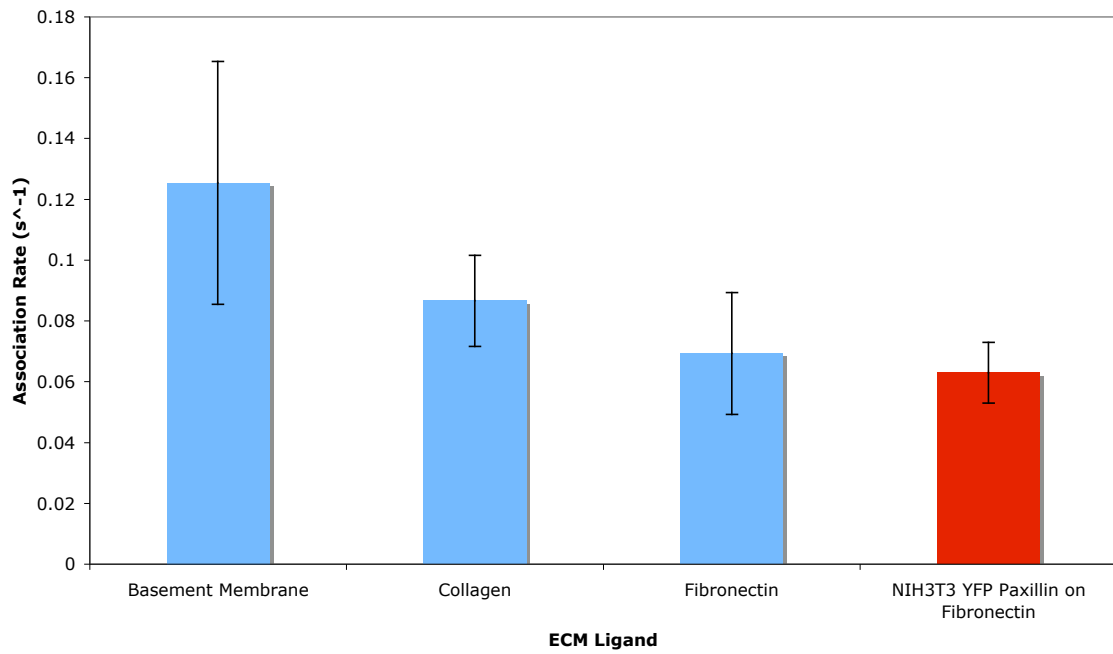
Figure 2.2. **MCF10A mCherry Paxillin Association Rate on ECM coated Glass.** *Blue bars represent calculated rate constant. Red bar represents value reported in literature for NIH3T3 YFP Paxillin on Fibronectin[50]. Error bars are +/- standard error.*

Discussion

The largest association rate for paxillin was determined to be 0.125 s^{-1} and occurred on the rBM substrate. The Association dynamics for paxillin on collagen represented a 33% decrease and paxillin on fibronectin a 55% reduction compared to paxillin on rBM. The association rate on fibronectin is expected to be the lowest because it is measuring the dynamics of paxillin in $\alpha_5\beta_1$ rich adhesions which are suspected to form stronger and longer lasting associations to the fibronectin substrate than $\alpha_2\beta_1$ would on collagen. The difference between collagen and rBM is unexpected and likely is a result of the large error associated with rBM. The reported results for NIH3T3 YFP-Paxillin on fibronectin coated glass [50] report a nearly identical association rate for my MCF10A mCherry-Paxillin on fibronectin coated glass. This similarity between a fibroblast and an epithelial cell suggests that the association rates measured for Paxillin are a general result not specific to the cells lines.

CHAPTER 3

Introduction

Integrins are implicated in cancer. Interestingly, data show that primary human breast tumors frequently exhibit a decrease in the expression of the 'differentiation-associated' laminin/collagen receptor α_2-integrin, but they often express the 'invasion and growth-linked' fibronectin receptor α_5-integrin [25]. Furthermore, there are known important mechanical differences between these two integrins. Studies have demonstrated $\alpha_5\beta_1$ forms 'catch bonds' with fibronectin giving it the ability to sustain higher mechanical loads which can also influence FAK signaling [22,28,43]. Thus I hypothesize these special mechanical properties confer to $\alpha_5\beta_1$ unique force sensing and transducing effects causing it to be enriched/selected for in tumors such as breast cancer. Because of these inherent capabilities it is important to determine the molecular mechanisms overseeing its regulation. Work on $\alpha_5\beta_1$ integrin recycling demonstrated it occurs very differently than $\alpha_v\beta_3$ hinting that $\alpha_5\beta_1$ turnover dynamics are possibly different than many other integrins, and in particular $\alpha_2\beta_1$ [48]. Thus integrin specificity may arise from differences between the dynamics of integrins.

To directly test this hypothesis I employed the optimized FRAP system to measure integrin specificity between the clustering dynamics of α_2-integrin on collagen coated glass and α_5-integrin on fibronectin coated glass.

In order to bend the investigation of integrin specificity and ECM rigidity towards increased understanding of these effects in breast cancer I chose to use the spontaneously immortalized non-transformed human mammary epithelial

MCF10A cell line. I have chose to use GFP-α_2-integrin and GFP-α_5-integrin as

they are the ideal constructs to use due to GFP exhibiting a lack of bleaching at

low laser intensity imaging and rapid extinguishment at intentional high laser

intensity bleaching.

Clearly the binding dynamics of integrins are distinct from paxillin in many

ways, most importantly they laterally assemble into clusters. Yet analysis of

integrin FRAP data can use the same equation characterizing the simplified

paxillin interactions by rationalizing integrin behavior in the following manner.

Any reduction in the free diffusion of integrins is indicative of binding reactions.

Therefore the possible binding interactions can be encompassed by three

different diffusion regimes (**Figure 3.1**). In the first regime the integrin dimer is

unbound undergoing nearly free 2D diffusion within the plane of the membrane.

The second scenario encompasses reduced diffusivity compared to free diffusion

when the integrin is bound by either a cytoskeletal adapter protein or an

extracellular ligand. Finally, the third case captures the most hindered state of

diffusion occurring when the integrin is bound on both sides of the membrane.

This hierarchy of mobility assumes different conformational states incur negligible

changes in diffusivity, and individually cytoskeletal connections or extracellular

attachments retard motion moderately while simultaneous binding above and

below the membrane reduce diffusivity dramatically. These assumptions

provided the basis for the simplified dynamic model [27] of integrin clustering and

recruitment to focal adhesions employed in this work (**Figure 3.2**). Here the

process of integrin clustering is governed by two first order reactions, the first

concerns the activation state of integrins and the second their reversible

aggregation within clusters. The three different conformational states (closed,

open-nonligand, open-ligand) are collapsed onto two reversible states,

Integrin$_{Closed}$ and Integrin$_{Open}$. The kinetic rate constants k_{act} and k_{inact} refer to

transitions of the integrin to the active and inactive states, respectively. Once

activated, integrins are recruited to clusters with the association rate constant k_{on}

and leave with the dissociation rate constant k_{off}. FRAP curves of integrins in

peripheral focal adhesions lack change upon forced integrin activation

suggesting the activation rate far exceeds the association rate. Therefore, it has

been asserted integrin association is the rate limiting step in cluster formation.

Under these conditions the recovery curve can be used to derive the integrin

association rate constant with the same analysis routines used to decipher

paxillin FRAP data.
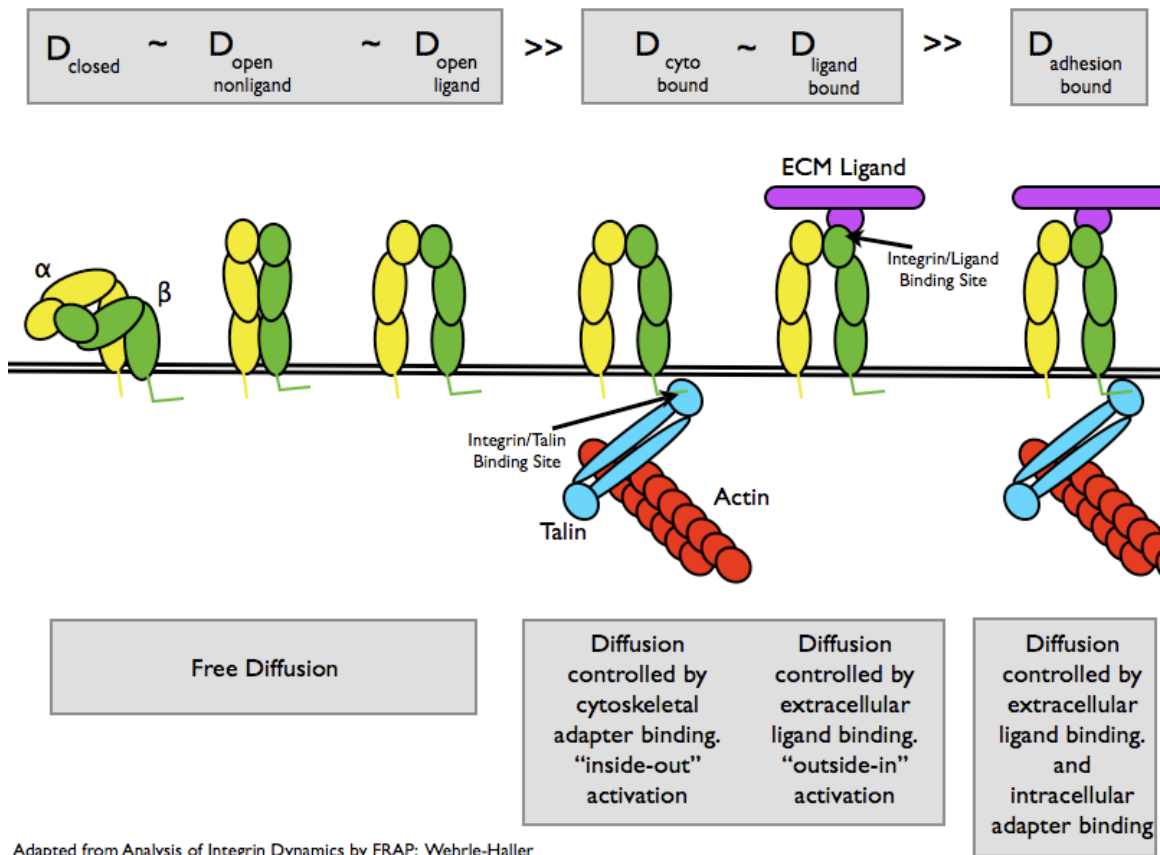
Figure 3.1. Integrin Diffusion Regimes. *Integrins can be envisioned to inhabit three different diffusion regimes. The left side shows the approximately free two-dimensional diffusion regime in which the three different conformational states of the integrin are assumed to contribute negligible changes in diffusivity. The middle region contains the moderately decreased diffusion regime in which the integrin is bound either on the cytoplasmic or the extracellular matrix side of the membrane but not both. The right section corresponds to the heavily reduced diffusion regime caused by the integrin being bound to both the cytoskeleton and the extracellular matrix. Adapter with permission from [27].*
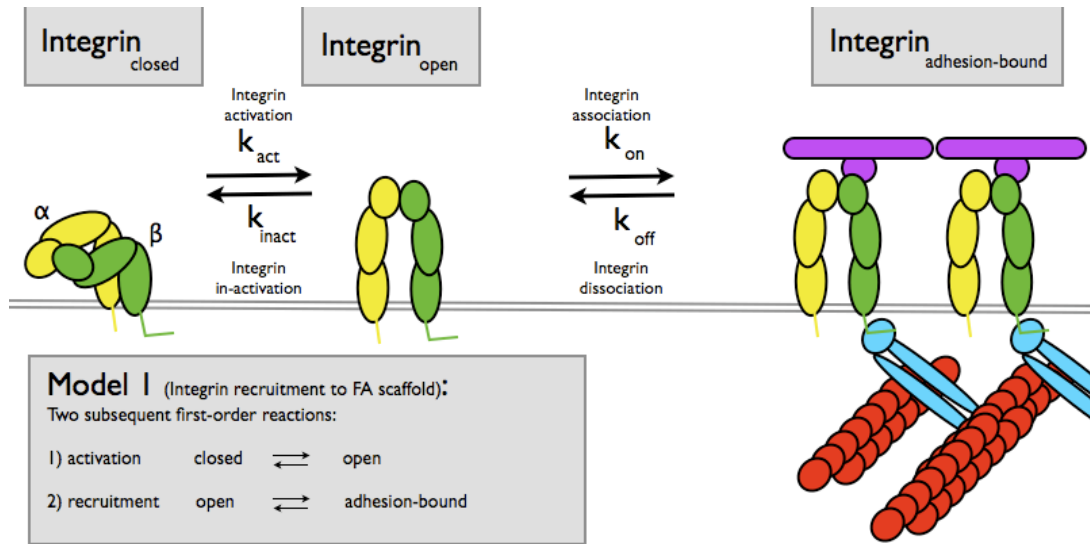
Figure 3.2. Kinetic Model of Integrin Clustering. *A condensed kinetic view of Figure CH3A. This dynamic model of integrin clustering employs two first-order reactions to capture the conformational transitions between active and inactive states, and the association/dissociation of an activated integrin from the cluster (adhesion). It is assumed that $k_{act} \gg k_{on}$ and k_{on} is therefore rate limiting. Thus the time rate of change of association is $k_{on}*[integrin_{open}]$ and the time rate of change of disssociation is $k_{off}*[integrin_{adhesion-bound}]$. Adapter with permission from [27].*

Results

I created both GFP-α_2-integrin and GFP-α_5-integrin constructs for the MCF10A mammary epithelial cell line. The GFP-α_2-integrin MCF10A cells were cultured on tissue culture plastic with a maximal passage number of 30 and displayed normal spreading and growth curves for the cell line. Confocal imaging of GFP-α_2-integrin showed good localization to focal adhesions with moderate expression levels. Similarly, GFP-α_5-integrin MCF10A cells were cultured on tissue culture plastic up to passage 30 and displayed healthy spreading and growth characteristics. However, confocal imaging of GFP-α_5-integrin showed subpar localization to focal adhesions and overall weak expression levels.   Due to these limitations use of the GFP-α_5-integrin construct was not used in experiments.

I successfully functionalized glass coverslips with collagen protein. The GFP-α_2-integrin MCF10A cells were seeded on the collagen slides 24 hours before each FRAP experiment. Cells readily divided and exhibited phenotypically normal spreading.
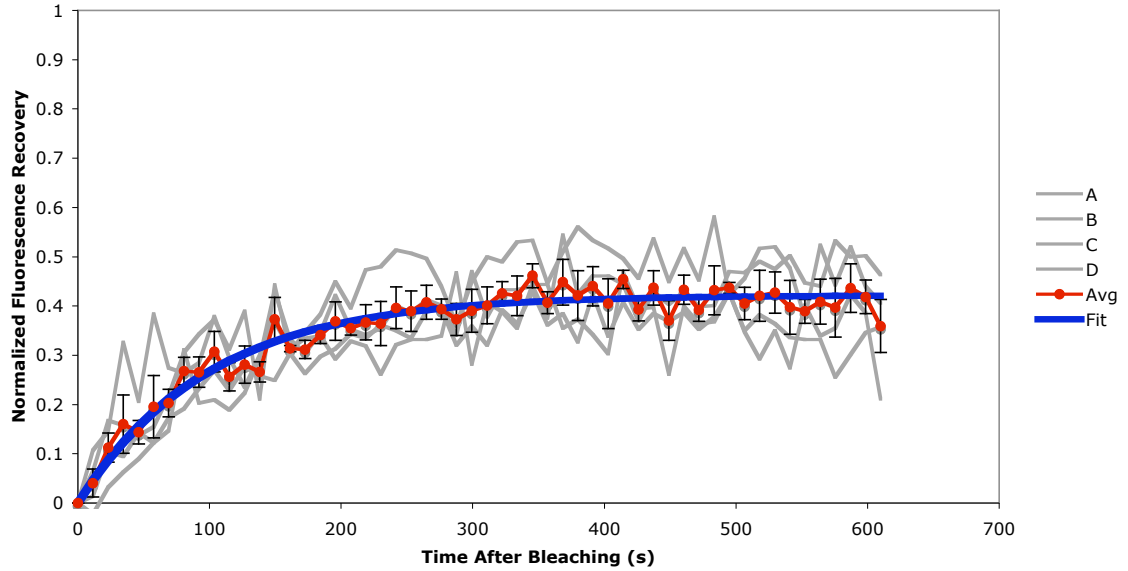
For GFP-α_2-integrin expressing MCF10A cells on collagen conjugated glass I calculated an α_2-integrin association rate of 0.010 s^{-1}, a half time of recovery of 69 s, and a mobile fraction of 42% **(Figure 3.1).**

FRAP of MCF10A GFP α2-integrin on collagen conjugated Glass

$K_{on} = 0.010 \text{ s}^{-1}$

$t_{1/2} = 69 \text{ s}$

Mobile Fraction = 42 %

Figure 3.3 **MCF10A GFP α₂-integrin Dynamics on Collagen coated Glass**. *Grey lines represent FRAP experiments performed on individual adhesions within different cells. Red line is average recovery curve of all experiments. Blue line represents fit of average curve according to Eq(6) (See Methods). Error bars are +/- standard error.*

Discussion

Prior FRAP work using NIH3T3 cells cultured on fibronectin conjugated glass reported a GFP-α_5-integrin association rate constant of 0.013 s^{-1} and a low mobile fraction near 20% [50]. I was unable to make comparisons between GFP-α_5-integrin in the MCF10A cell line because the construct exhibited low expression levels and poor localization into adhesion structures. It was difficult to make meaningful comparisons of clustering dynamics between NIH3T3 GFP-α_5-integrin and MCF10A GFP-α_2-integrin as it was a comparison between fibroblasts and epithelial cells with different types of integrins. Nonetheless, a comparison was made by normalizing the integrin association rates to the paxillin association rates within each cell line. The work using NIH3T3 cells on fibronectin reported YFP-Paxillin had an association rate constant of 0.069 s^{-1} with a mobile fraction near 70%. Therefore the association rate for NIH3T3 GFP-α_5-integrin was approximately ~20% of the NIH3T3 YFP-Paxillin association rate. For my experiments the association rate for MCF10A GFP-α_2-integrin was ~12% of the association rate of MCF10A-mCherry-Paxillin on collagen coated glass. Using this relative scale I reported a slight increase in the clustering dynamics of α_5-integrin compared to α_2-integrin. It is difficult to determine whether this minor difference brings with it phenotypic consequences to cell behavior. The main conclusion of these experiments was that similarities between the relative integrin association rates for the two cell lines suggests that my FRAP system provided at least a reasonable estimate of the clustering dynamics of α_2-integrin

within focal adhesions in a nonmalignant breast cell line when cultured on ECM

conjugated glass.

CHAPTER 4

Introduction

Remodeling of the extracellular matrix (ECM) occurs through a process in which ECM molecules interact with clusters of integrin receptors to generate signaling cascades transmitted from the cytoskeleton to the nucleus [10]. The resulting expression of genes then affects the composition and organization of the ECM in a reciprocal process [40]. Disruptions and perturbations to this network results in a loss of cell and tissue homeostasis resulting in a number of diseases including breast cancer. For example, mammary epithelial cells (MECs) when grown in soft ECMs of compliance similar to normal mammary gland develop into milk duct like structures called acini, but when grown on tumor-stiff ECMs they create aberrant malignant structures [7]. Additionally, recent work using mice reported in an oncogene-initiated epithelium exogenous ECM stiffening by crosslinking promotes focal adhesions, enhances signaling, and induces invasion. And in the premalignant epithelium inhibition of integrin signaling represses invasion while forced integrin clustering promotes focal adhesions and drives invasion into a stiffened ECM [24]. Thus ECM stiffness as perceived by integrins regulates the transition from tissue homeostasis to malignancy.

Recent work has demonstrated that endocytosis and recycling of integrins acts to promote the turnover of focal adhesions when cells migrate on 2D surfaces and endocytic trafficking of integrins directly contributes to an invasive phenotype analogous to metastatic tumors [52,53]. Studies also suggest that

downstream integrin signaling is influenced by the manner in which they are trafficked. [51] As such, I hypothesized that stiffness alters integrin turnover dynamics and consequently drives improper signaling.

To test the hypothesis that ECM rigidity regulates integrin dynamics I used my FRAP system to investigate α_2-integrin clustering kinetics across a spectrum of substrate compliances.

Polyacrylamide gels functionalized with collagen protein were chosen to create 2D substrates for the culture of GFP-α_2-integrin expressing MC10A cells. I chose polyacrylamide because it is an excellent material for the culture of MECs since it is biocompatible, non-toxic, resistant to non-specific absorption of proteins, and optically clear for microscopy applications. Moreover, mechanical stiffness of polyacrylamide substrates can be precisely modulated by adjusting the concentrations of acrylamide or bis-acrylamide prior to polymerization [30]. Polyacrylamide substrates were fabricated of varying rigidity to recapitulate the range of stiffness between normal mammary gland and tumors [3]. The chosen range of gel stiffness was: 0.6kPa, 6kPa, 13.8kPa, and 22kPa. The following is the rational for inclusion of each compliance: the 0.6kPa gel is in the range of normal mammary tissue compliance, the 6kPa and 13.8kPa gels comprise the low and high end of pathological breast tissue compliance, and the 22 kPa gel is near the compliance of pathological lung tissue.
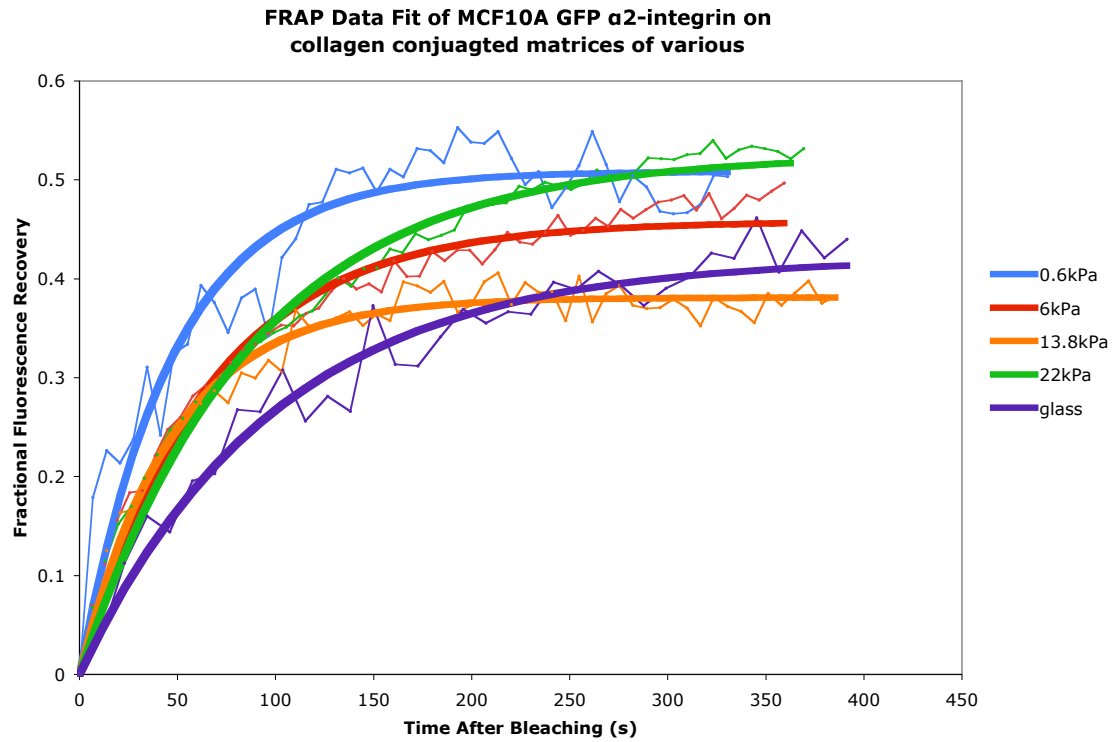
Results

      I successfully cast each stiffness of polyacrylamide gel and functionalized it with collagen protein. The GFP-α_2-integrin MCF10A cells were seeded on the collagen coated gels 24 hours before each FRAP experiment. Cells readily divided and spread on each gel with only the most compliant gel routinely containing a small percentage of non-adherent cells. Stiffer substrates exhibited greater amounts of spreading, indicating these MECs were responsive to this range of substrate stiffness.

      FRAP experiments using GFP-α_2-integrin expressing MCF10A cells were carried out on each of the proposed gels. I calculated the following results for GFP-α_2-integrin on the individual gels. On the 0.6kPa gel α_2-integrin had an association rate of 0.021 s^{-1}, a half time of recovery of 33 s, and a mobile fraction of 51%. On the 6kPa gel α_2-integrin had an association rate of 0.015 s^{-1}, a half time of recovery of 45 s, and a mobile fraction of 46%. On the 13.8kPa gel α_2-integrin had an association rate of 0.021 s^{-1}, a half time of recovery of 33 s, and a mobile fraction of 38%. Finally, on the 22kPa gel α_2-integrin had an a association rate of 0.011 s^{-1}, a half time of recovery of 60 s, and a mobile fraction of 52% **(Figure 4.1 & 4.2 & 4.3).**
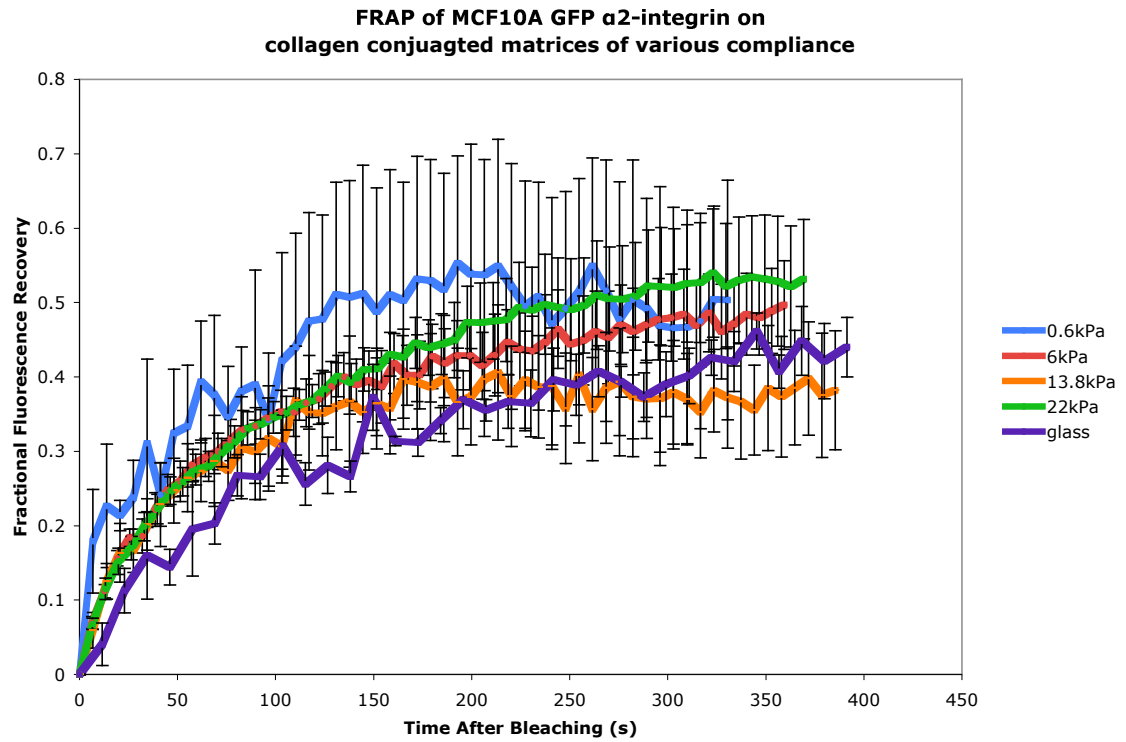
Figure 4.1. MCF10A GFP α$_2$-integrin Dynamics on Collagen conjugated Gels.
Lines represent average recovery curve of multiple adhesions for a single gel compliance. Error bars are +/- standard error.

FRAP Data Fit of MCF10A GFP α2-integrin on collagen conjuagted matrices of various

Legend:
- 0.6kPa
- 6kPa
- 13.8kPa
- 22kPa
- glass

X-axis: Time After Bleaching (s)
Y-axis: Fractional Fluorescence Recovery

Figure 4.2. **MCF10A GFP α₂-integrin Recovery Fit on Collagen conjugated Gels.** *Thin lines represent average recovery curve of multiple adhesions for a single gel compliance. Thick lines represent fit of average curve according to Eq(6) (See Methods).*

**MCF10A GFP α2-Integrin
Association Rate Constant Rate vs ECM stiffness**
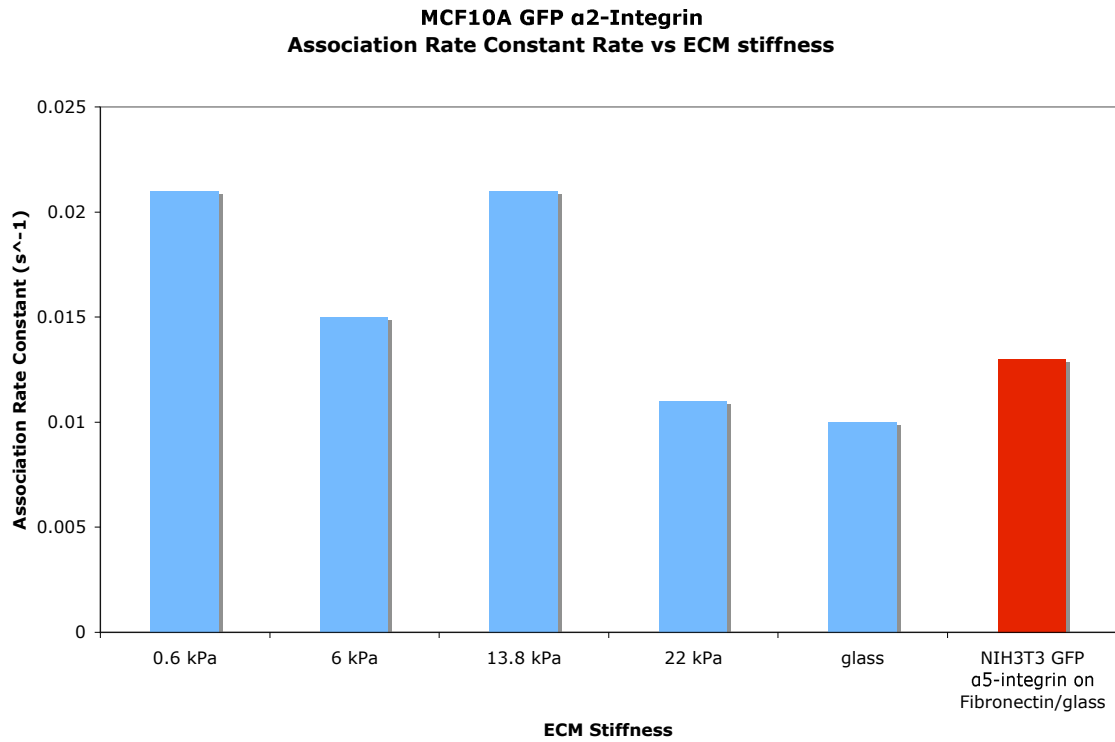
Figure 4.3. **MCF10A GFP α2-integrin Association Rate on Collagen conjugated Gels**. *Blue bars represent value of calculated association rate constant for MCF10A GFP-α2-integrin on collagen crosslinked gels of indicated compliance. Red bar represents value of association rate constant reported in literature for NIH3T3 GFP-α5-integrin on Fibronectin coated glass [50].*

Discussion

A simple interpretation of this data depends on rationalization of the standard error for a particular compliance. It could be the case that greater sampling would prove the association rate on the 13.8kPa gel is at the lower value of its standard error bar. If this were true, then it would suggest α_2-integrin clustering dynamics decrease as the matrix becomes stiffer. Provocatively, this trend suggests the existence of a switching point in tissue phenotype based on matrix rigidity where the association rate of α_2-integrin into the focal adhesion drops sufficiently low to drive pathology. Thus, assuming the dissociation rate is not affected, a lowered association rate implies a decrease in cluster size that could lead to disassembly of the adhesion. If α_2-integrin activity influences its own expression level this could explain why α_2-integrin is often expressed at lower levels in primary breast cancers. Clearly this claim is softened by the fairly large deviations present within each recovery curve and therefore association rate constant estimate.

Interestingly, increasing matrix stiffness from normal mammary compliance to drastically beyond tumor stroma does not appear to alter α_2-integrin clustering dynamics by an amount immediately recognizable as impacting cell behavior. However, biological signaling is built on circuits which amplify their effects and so it may be the case that a 50% increase in α_2-integrin association rate corresponds to a dramatic change in outcome. Additionally, there may be an intrinsic aspect to integrin clustering such that the association

dynamics occur over a finite range that is always above a certain threshold and overall dynamics are instead dictated by the dissociation rate.

Previous work has indicated 1kPa as the compliance above which integrin clusters mature into larger and more numerous adhesions. It is thus no surprise the 0.6kPa gel also produced the least defined adhesions and consequently exhibited the largest standard error in recovery dynamics. However, because all α_2-integrin association rates measured on gels were only 10% to 50% greater than the value reported for α_2-integrin on glass it suggests that the values are consistent and reasonable **(Figure 4.3)**. Therefore, I conclude the experiments produced valid and consistent numbers for α_2-integrin clustering dynamics but the relationship between kinetic rates of bond formation and increasing matrix stiffness remains an open question.

CHAPTER 5

Discussion

Evidence suggests that primary cell-ECM receptors known as integrins drive different cell and tissue level behaviors and consequently also contribute non uniformly to their pathologies [17,24,42,52]. Studies have demonstrated a link between integrins, increased matrix stiffness, and breast cancer [24]. In particular $\alpha_5\beta_1$ is elevated in breast cancers and is known to drive invasion where as $\alpha_2\beta_1$ is reduced in breast cancers and is thought to contain tumor suppressor properties, suggesting integrin specificity in breast cancer [25]. Studies have demonstrated $\alpha_5\beta_1$ forms 'catch bonds' with fibronectin giving it the ability to sustain higher mechanical loads which can also influence FAK signaling [22,43]. Thus I hypothesized these conferred upon $\alpha_5\beta_1$ unique force sensing and transducing effects resulting in it being enriched/selected for in tumors such as breast cancer. Because of the potency $\alpha_5\beta_1$ exhibits it is important to determine the molecular mechanisms overseeing its regulation. Work on $\alpha_5\beta_1$ integrin recycling demonstrated it occurs very differently than $\alpha_v\beta_3$ hinting that $\alpha_5\beta_1$ turnover dynamics are possibly different than many other integrins, and in particular $\alpha_2\beta_1$ [48] The idea being integrin specificity may be related to the dynamics of the integrins. Thus I used the high resolution optical imaging technique of FRAP to determine if the turnover dynamics were different between the two integrins and in particular probed how their individual dynamics changed on soft (normal) and stiff (pathologic) ECM substrates.

The main question about integrin turnover dynamics underlying integrin specificity remains unanswered because of experimental difficulties encountered with MCF10A GFP-α_5-Integrin. The cell line exhibited normal growth and spreading but GFP-α_5-Integrin had low expression levels in addition to poor localization into adhesions and consequently was productive in experiments. Thus I was not able to compare α_5-integrin to α_2-integrin and investigate integrin specificity directly. I was able to probe integrin specificity indirectly by comparing MCF10A mCherry-Paxillin association rates on glass coated with either fibronectin, collagen, or rBM. My calculation for the paxillin association rate was highest on the rBM, 33% lower on collagen, and 55% lower on fibronectin. This trend fits nicely within the context of the $\alpha_5\beta_1$ fibronectin catch bond making $\alpha_5\beta1$ integrin bind in a longer and stronger than $\alpha_2\beta_1$ on collagen. Thus their is support that α_5-integrin has slower turnover dynamics than α_2-integrin which may contribute to integrin specificity.

I successfully completed FRAP experiments quantifying the association dynamics of α_2-integrin within focal adhesions in the nonmalignant MCF10A cell line on matrices of increasing stiffness. An immediately obvious functional relationship between matrix rigidity and α_2-integrin association dynamics was not uncovered. Instead I observed an apparent decrease in association rate as stiffness increase, except for a spike at the 13.8kPa gel (upper bound compliance for pathologic breast tissue). The large error margin associated with this outlier suggests experimental replication may constrain the data point so it lies on the trend of increasing stiffness and decreasing association rate. If true,

and assuming a constant dissociation rate it suggests a possible mechanism by which a fibrotic matrix acts to disassemble $\alpha_2\beta_1$ adhesions counteracting their tumor suppressor properties and providing a rationale for their decreased expression levels in primary breast cancer.

Future Directions

Clearly the main issue to confront is the successfull production of MCF10A GFP-α_5-Integrin. It was uncertain as to why GFP-α_5-Integrin was poorly recruited into adhesion but was assumed to be due steric hinderance caused by the fluorophore and its tether. FRAP studies can also use YFP and so that may be a valid choice if future work continues to struggle with adhesion localization issues. Essential to a better interpretation of the data is knowledge of the dissociation rates. Obviously only having information about the association rate of a process does not inform about the overall amount of increase or decrease, for that the removal rate is also required. Thus knowing rates for both sides of the binding equation are essential because the dissociation rate may be functionally linked to increased matrix stiffness, but regardless it is clearly a valid parameter for distinguishing between α_5-Integrin and α_2-Integrin and hence could illuminate the role of integrin specificity in the transition from tissue homeostasis and malignancy in the breast.

Bibliography

1. Xu R, Boudreau A, Bissell MJ. Tissue architecture and function: dynamic reciprocity via extra- and intra-cellular matrices. Cancer and Metastasis Reviews. 2009;**28**:167-176.
2. Desprat N, Supatto W, Pouille PA, Beaurepaire E, Farge E . Tissue Deformation Modulates Twist Expression to Determine Anterior Midgut Differentiation in Drosophila Embryos. Developmental cell. 2008;**15**:470-477.
3. Yu H, Mouw JK, Weaver VM. Forcing form and function: biomechanical regulation of tumor evolution. Trends in Cell Biology. 2011:**21**:47-56.
4. Schwartz M. The Extracellular Matrix: Integrins and Extracellular Matrix in Mechanotransduction. Cold Spring Harbor Perspectives in Biology 2010:**2;**12
5. Kumar S, Weaver V. Mechanics, malignancy, and metastasis: The force journey of a tumor cell. Cancer and Metastasis Reviews. 2008;**28**:113-127
6. Georges PC, Miller WJ, Meaney DF, Sawyer E, Janmey P. Matrices with compliance comparable to that of brain tissue select neuronal over glial growth in mixed cortical cultures. Biophysical Journal. 2006;**90**:3012–3018.
7. Paszek MJ, Zahir N, Johnson KR, Lakins JN, Rozenberg GI, Gefen A, Reinhart-King CA, Margulies SS, Dembo M, Boettiger D, Hammer DA, Weaver VM. Tensional homeostasis and the malignant phenotype.Cancer Cell. 2005;**8**(3):241-54.
8. *Jaalouk DE, Lammerding J. Mechanotransduction gone awry. Nature Reviews Molecular Cell Biology.2009;**10**:63-73*
9. Lansman JB, Hallam TJ, Rink TJ. Single stretch-activated ion channels in vascular endothelial cells as mechanotransducers?. Nature. 1987;**325**:811-813
10. Wang N, Tytell J.D, Ingber D.E. Mechanotransduction at a distance: mechanically coupling the extracellular matrix with the nucleus. *Nature Reviews Molecular Cell Biology*. 2009;**10**:75-82.
11. contractility and G protein-linked receptor stimulation
12. Paszek MJ. Integrins sense extracellular-matrix rigidity to regulate mammary-epithelial tissue phenotype. (January 1, 2009). *Dissertations available from ProQuest.*Paper AAI3381773.
13. Barczyk H, Carracedo S, Gullberg D. Integrins. Cell Tissue Research. 2010;**339**(1):269–280.
14. Luo BH, Carman CV, Springer TA. Structural basis of integrin regulation and signaling. Annual Review Immunololgy.2007;**25**:619-647
15. Cluzel C, Saltel F, Lussi J, Paulhe F, Imhof BA, Wehrle-Haller B. The mechanisms and dynamics of αvβ3 integrin clustering in living cells. Journal Cell Biology. 2005;**171**:383-392.
16. Hynes RO. Integrins: bidirectional, allosteric signaling machines. Cell. 2002;**110**:673-687.
17. Liddington RC, Ginsberg MH. Integrin activation takes shape. Journal Cell Biology.2002;**158**:833-839.
18. Berrier AL, Yamada KM. Cell-matrix adhesion. Journal Cell Physiology. 2007; **213**: 565–573.

19. Cavalcanti-Adam EA, Volberg T, Micoulet A, Kessler H, Geiger B. Cell spreading and focal adhesion dynamics are regulated by spacing of integrin ligands. Biophysical Journal. 2007; **92**: 2964–2974.

20. Massia SP, Hubbell JA. An RGD spacing of 440 nm is sufficient for integrin alpha V beta 3-mediated fibroblast spreading and 140 nm for focal contact and stress fiber formation. Journal Cell Biology. 1991; **114**: 1089–1100.

21. Kato M, Mrksich M. Using model substrates to study the dependence of focal adhesion formation on the affinity of integrin-ligand complexes. Biochemistry. 2004; **43**: 2699–2707.

22. Kong F, Garcia AJ, Mould AP, Humphries MJ, Zhu C. Demonstration of catch bonds between an integrin and its ligand. Journal Cell Biology.2009;185:1275–1284.

23. Macdonald A, Horwitz AR, Lauffenburger DA. Kinetic model for lamellipodal actin-integrin 'clutch' dynamics. Cell Adhesion Migration. 2008;**2**(2): 95–105.

24. Levental KR, Yu H, Kass L, Lakins JN, Egeblad M, Erler JT, Fong S, Csiszar K, Giaccia A, Weninger W, Yamauchi M, Gasser DL, Weaver VW. Matrix Crosslinking Forces Tumor Progression by Enhancing Integrin Signaling. Cell. 2009;**139**(5):891-906

25. Chrenek M, Wong PW, Weaver VM. Integrins and cell adhesions as modulators of mammary cell survival and transformation. Breast Cancer Research. 2001;**3**:224-229.

26. Paszek MJ, Boettiger D, Weaver VM, Hammer DA. Integrin clustering is driven by mechanical resistance from the glycocalyx and the substrate. PLoS computational biology. 2009;**5**(12)

27. Wehrle-Haller B, Imhof BA. The inner lives of focal adhesions. Trends in Cell Biology. 2002;**12**(8):382-389.

28. Roca-Cusachsa P, Gauthiera NC, del Rioa A, Sheetz MP. Clustering of α5β1 integrins determines adhesion strength whereas αvβ3 and talin enable mechanotransduction. PNAS.2009(**106**)(38):16245-16250

29. Soule HD, Maloney TM, Wolman SR, Peterson WD Jr, Brenz R, McGrath CM, Russo J, Pauley RJ, Jones RF, Brooks SC. Isolation and characterization of a spontaneously immortalized human breast epithelial cell line, MCF-10. Cancer Research. 1990; **50**: 6075-6086.

30. Pelham RJ, Wang Y. Cell locomotion and focal adhesions are regulated by substrate flexibility. Proceedings Natlonal Academy Science. 1997;**94**:13661-13665.

31. Pless DD, Lee YC, Roseman S, Schnaar RL. Specific cell adhesion to immobilized glycoproteins demonstrated using new reagents for protein and glycoprotein immobilization. Journal Biological Chemistry.1983;**258**:2340–2349.

32. Axelrod D, Koppel DE, Schlessinger J, Elson E, Webb WW. Mobility measurement by analysis of fluorescence photobleaching recovery kinetics. Biophys Journal. 1976;**16**:1055-69.

33. Sprague BL, Pego RL, Stavreva DA, McNally JG. Analysis of Binding Reactions by Fluorescence Recovery after Photobleaching. Biophysical Journal. 2004;**86**(6):3473-3495.

34. McNally JG. Quantitative FRAP in Analysis of Molecular Binding Dynamics In Vivo. Fluorescent Proteins Methods in Cell Biology.2008;**85**:329-351.

35. Lippincott-Schwartz J, Snapp E, Kenworthy A. Studying protein dynamics in living cells. Nature Reviews Molecular Cell Biology. 2001;**2**:444-456.

36. Carrero G, Crawford E, Hendzel MJ, de Vries G. Characterizing fluorescence recovery curves for nuclear proteins undergoing binding events. Bulletin Mathematical Biology.2004;**66**:1515-1545.

37. Hinow P, Rogers CE, Barbieri CE, Pietenpol JA, Kenworthy AK, DiBenedetto E. The DNA binding activity of p53 displays reaction-diffusion kinetics. Biophysics Journal.2006;**91**:330-34.

38. Lele T, Oh P, Nickerson JA, Ingber DE. *An improved mathematical model for determination of molecular kinetics in living cells with FRAP*. Mechanics & Chemistry of Biosystems. 2004;**1**:181-190.

39. Hynes RO. The Extracellular Matrix: Not Just Pretty Fibrils. *Science.* 2009; **326**:1216-1219.

40. Vogel V, Sheetz MP. Cell fate regulation by coupling mechanical cycles to biochemical signaling pathways. *Current Opinion in Cell Biology.* 2009; **21**:38-46.

41. Lodish H, S AB, Zipursky L, Matsudaira P, Baltimore D, Darnell J. Molecular Cell Biology, 4th edition. 2000 (W. H. Freeman, New York).

42. Singh P, Carraher C, Schwarzbauer JE. Assembly of Fibronectin Extracellular Matrix. Annual Review of Cell and Developmental Biology.2010; **26**: 397-419

43. Friedland JC, Lee MH, Boettiger D. Mechanically Activated Integrin Switch Controls α5β1 Function. Science;**323**(5914):642-644.

44. .Moore KA. Control of embryonic lung branching morphogenesis by the Rho activator, cytotoxic necrotizing factor 1. Journal Surgical Research. 2002.**104**:95–100.

45. Miao H. EphA kinase activation regulates HGF-induced epithelial branching morphogenesis. Journal Cell Biology.2003;**162**:1281–1292.

46. Butler LC. Cell shape changes indicate a role for extrinsic tensile forces in Drosophila germ-band extension. Nature Cell Biology.2009;**11**:859–864.

47. .Frantz C, Stewart KM, Weaver VM. The extracellular matrix at a glance. Journal of Cell Science. 2010;**123**(24):4195-200.

48. White DP, Caswell PT, Norman JC. αvβ3 and α5β1 integrin recycling pathways dictate downstream Rho kinase signaling to regulate persistent cell migration. JCB.2007;**177**(3): 515-525.

49. Turner CE, Glenney JR, Burridge K. Paxillin: a new vinculin-binding protein present in focal adhesions. J Cell Biology. 1990;111:1059-1068

50. Humphries JD, Wang P, Streuli C, Geiger B, Humphries MJ, Ballestrem C. Vinculin controls focal adhesion formation by direct interactions with talin and actin. JCB.2007;179(5):1043-1057.

51. Caswell PT, Norman JC. Integrin trafficking and the control of cell migration. Traffic.2006;**7**:14–21.

52. Valdembri D. Neuropilin-1/GIPC1 signaling regulates 51 integrin traffic and function in endothelial cells. PLoS Biology.2009;7:e25.

53. Caswell PT, Spence HJ, Parsons M, White DP, Clark K, Cheng KW, Mills GB, Humphries MJ, Messent AJ, Anderson KI, McCaffrey MW, Ozanne1 BW, Norman JC. Rab25 Associates with α5β1 Integrin to Promote Invasive Migration in 3D Microenvironment. Developmental Cell. 2007;**13**(4):496-510 .

UCSF Library Release

Publishing Agreement

It is the policy of the University to encourage the distribution of all theses and dissertations. Copies of all UCSF theses and dissertations will be routed to the library via the Graduate Division. The library will make all theses and dissertations accessible to the public and will preserve these to the best of their abilities, in perpetuity.

Please sign the following statement:

I hereby grant permission to the Graduate Division of the University of California, San Francisco to release copies of my thesis or dissertation to the Campus Library to provide access and preservation, in whole or in part, in perpetuity.

April,02,2011

_____   _____

Author Signature   Date